

# Nonlinear Seismic Analysis of Base-Isolated Reactor Building by the Hybrid Frequency-Time-Domain Procedure

Georges R. Darbe  
*University of California, Berkeley, CA USA*

## INTRODUCTION

A sliding-type base isolation system can be used to isolate a reactor building from a seismic excitation. The seismic analysis of this type of structure is a challenging task when the radiation condition in the supporting soil must be appropriately accounted for. The reason is that the nonlinear effects of the sliding-type isolation mechanism are defined in the time domain while the contribution of the semi-infinite soil medium to the equation of motion is defined in the frequency domain. One way of performing the seismic analysis of a nonlinear structure interacting with a soil medium characterized by frequency-dependent stiffness coefficients is to disregard the frequency dependence of the stiffness coefficients of the soil. The soil is thus replaced by a set of springs and dashpots with constant coefficients. A time-stepping algorithm can then be used to solve the equation of motion. This approach is obviously only approximate and the results of the analysis performed in this fashion are not as accurate as the results obtained in a linear soil-structure interaction analysis in which the frequency-dependence of the soil contribution is duly accounted for.

In this paper, it is shown how the nonlinear seismic analysis of a base-isolated reactor building is performed when duly accounting for the frequency-dependence of the soil contribution to the equation of motion. The same degree of accuracy is then achieved as when performing a linear soil-structure interaction analysis in which this frequency dependence is considered. The nonlinear analysis is performed using the hybrid-frequency-time domain (HFTD) procedure which proves to be very effective in handling this type of problem.

## SYSTEM INVESTIGATED: REACTOR BUILDING ON SLIDING-TYPE BASE ISOLATION

Model: The two-dimensional model of a reactor building on a sliding-type base isolation system shown in Fig. 1 is used to obtain the global response in a multistep seismic analysis. The reactor building with internals is modeled by beams and lumped masses. This superstructure rests on a rigid upper raft which is connected to a rigid lower raft through the isolation mechanism. The lower raft is bound to the soil.

Superstructure: The dynamic properties of the superstructure are characterized by fixed-base natural frequencies of 4.6 Hz for the fundamental frequency, 7.9 Hz for the second frequency and 14.4 Hz for the third frequency. The energy dissipation within the superstructure is taken as stiffness proportional with

$$[C] = 0.01 \text{ sec } [K] \text{ (5% critical damping at 1.6 Hz).}$$

Isolation mechanism: The horizontal force/displacement relation of the sliding-type isolation mechanism is given by the elasto-plastic relation shown in Fig. 2. It is defined by the stiffness coefficient  $k_h = 2 \times 10^9 \text{ N/m}$  and the sliding force  $R_h = 60 \times 10^6 \text{ N}$ . A viscous type of energy dissipation also occurs, with  $c_h = 0.015 \text{ sec } k_h$ . In the rocking direction, the moment/rotation relation is linear-

elastic with the stiffness coefficient  $k_r = 150 \cdot 10^{12}$  Nm characterizing the relation. A viscous damper with  $c_r = 0.015$  sec  $k_r$  is also present. The three lowest small-amplitude natural frequencies of the superstructure and isolation mechanism on rigid soil are 1.0 Hz, 4.8 Hz and 8.9 Hz, respectively.

Soil: The soil consists of a layer of depth equal to the radius of the foundation (17.5 m) resting on a semi-infinite halfspace. The properties of the layer are: shear modulus of  $180 \cdot 10^6$  N/m<sup>2</sup>, mass density of  $2 \cdot 10^3$  kg/m<sup>3</sup> ( $C_s = 300$  m/s), Poisson's ratio of 1/3 and hysteretic damping ratio of 5%. The properties of the halfspace differ only in the value of the shear modulus equal to  $720 \cdot 10^6$  N/m<sup>2</sup> ( $C_s = 600$  m/s). The frequency-dependent stiffness coefficients characterizing the response of a massless circular rigid foundation welded to the layer are shown in Fig. 3. The stiffness coefficients form the 2x2 dynamic stiffness matrix  $[S_{bb}(\omega)]_g = [K_{bb}(\omega)]_g + i\omega [C_{bb}(\omega)]_g$ . The elements of  $[K_{bb}(\omega)]_g$  are normalized with respect to the corresponding static values of  $K_{hh} = 20 \cdot 10^9$  N/m,  $K_{rr} = 4.6 \cdot 10^{12}$  Nm and  $K_{hr} = K_{rh} = 13 \cdot 10^9$  N (the coupling coefficient is divided by 5 in the figure for better representation). The elements of  $[C_{bb}(\omega)]_g$  are normalized through multiplication by  $C_s/a$  (shear wave velocity of layer divided by foundation radius) and division by the static value of the corresponding spring coefficient.

Seismic input: The vertically propagating input earthquake is given by the horizontal free-surface acceleration time history of Fig. 4 with a peak acceleration of 30% g.

#### METHOD OF ANALYSIS: HFTD PROCEDURE

The hybrid-frequency-time domain (HFTD) procedure has been presented in details elsewhere (Darbre, 1988a; Kawamoto, 1983) and only its fundamental concept as well as those implementation details pertinent to the present analysis are presented here.

Fundamental Concept: In the HFTD procedure, the nonlinear system which needs to be analyzed is replaced by a linear system. Because it is linear, this latter system can be analyzed in the frequency domain and any frequency-dependent quantity can be duly accounted for. The linear system which is introduced differs from the nonlinear system which needs to be analyzed. The resulting difference in response is replaced by the response produced by pseudo-forces. The latter depend on the response itself and the problem has thus to be solved iteratively. Symbolically, the procedure is written as (Darbre, 1988b):

$$\begin{array}{ccc} \overbrace{\{F_{internal}\}} & = & \{F_{external}\} \\ \{F_{internal}\}_{linear} + \{\Delta F_{internal}\}_{nonlinear} & & \\ \\ \{F_{internal}\}_{linear} & = & \{F_{external}\} - \{\Delta F_{internal}\}_{nonlinear} \\ | & & | \\ \text{solved in} & & \text{defined in} \\ w\text{-domain} & & t\text{-domain} \\ | & & | \\ & & \text{evaluated in} \\ & & t\text{-domain} \end{array}$$

Implementation of procedure for system investigated: In this application, the pseudo-linear system is selected as the whole system with a non-sliding isolation mechanism (linear behavior). The equation of motion in the frequency domain is thus (in terms of total displacements):

$$\left[ \begin{array}{cc} [S_{ss}(\omega)]_s & [S_{sb}(\omega)]_s \\ [S_{bs}(\omega)]_s & [S_{bb}(\omega)]_s + [S_{bb}(\omega)]_g \end{array} \right] \left\{ \begin{array}{c} \{u_s(\omega)\} \\ \{u_b(\omega)\} \end{array} \right\} = \left\{ \begin{array}{c} \Omega(\omega) \\ 0 \end{array} \right\} + \left\{ \begin{array}{c} 0 \\ [S_{bb}(\omega)]_g \{u_b(\omega)\}_g \end{array} \right\}$$

The elements of the matrices identified by the subscript s outside of the brackets refer to the structure composed of the superstructure, the pseudo-linear isolation mechanism and the rafts, while  $[S_{bb}]_g$  refers to the dynamic stiffness of the massless foundation welded to the soil.  $\{u_b\}_g$  is the input motion identified earlier.

The nonlinear effects are collected in the vector of pseudo forces  $\{Q(\omega)\}$ . The vector  $\{Q(\omega)\}$  is the Fourier transform of the time-dependent vector  $\{Q(t)\}$ . Only two elements of this vector are non-zero, namely those referring to the degrees of freedom affected by the nonlinear sliding-type mechanism (horizontal direction of nodes 1 and 7). They are

$$\begin{Bmatrix} Q_{1h}(t) \\ Q_{7h}(t) \end{Bmatrix} = \begin{Bmatrix} (F_{1h}(t))_{\text{linear}} - (F_{1h}(t))_{\text{nonlinear}} \\ (F_{7h}(t))_{\text{linear}} - (F_{7h}(t))_{\text{nonlinear}} \end{Bmatrix}$$

where  $(F_{1h})_{\text{linear}}$  and  $(F_{7h})_{\text{linear}}$  are simply given by

$$\begin{Bmatrix} (F_{1h})_{\text{linear}} \\ (F_{7h})_{\text{linear}} \end{Bmatrix} = k_h \begin{bmatrix} 1 & -1 \\ -1 & 1 \end{bmatrix} \begin{Bmatrix} u_{1h} \\ u_{7h} \end{Bmatrix} + c_h \begin{bmatrix} 1 & -1 \\ -1 & 1 \end{bmatrix} \begin{Bmatrix} \dot{u}_{1h} \\ \dot{u}_{7h} \end{Bmatrix}$$

and where  $(F_{1h})_{\text{nonlinear}}$  and  $(F_{7h})_{\text{nonlinear}}$  are conveniently written as

$$\begin{Bmatrix} (F_{1h})_{\text{nonlinear}} \\ (F_{7h})_{\text{nonlinear}} \end{Bmatrix} = \begin{Bmatrix} (\bar{F}_{1h})_{\text{nonl.}} \\ (\bar{F}_{7h})_{\text{nonl.}} \end{Bmatrix} + c_h \begin{bmatrix} 1 & -1 \\ -1 & 1 \end{bmatrix} \begin{Bmatrix} \dot{u}_{1h} \\ \dot{u}_{7h} \end{Bmatrix}$$

The first part of the right-hand side of this latter equation refers to the stiffness contribution of the isolation mechanism while the second part refers to the viscous-damping contribution. The stiffness contribution is

$$(\bar{F}_{1h}(t+\Delta t))_{\text{nonl.}} = (\bar{F}_{1h}(t))_{\text{nonl.}} + k_h ((u_{1h}(t+\Delta t) - u_{7h}(t+\Delta t)) - (u_{1h}(t) - u_{7h}(t)))$$

$$(\bar{F}_{7h}(t+\Delta t))_{\text{nonl.}} = (\bar{F}_{7h}(t))_{\text{nonl.}} + k_h ((u_{7h}(t+\Delta t) - u_{1h}(t+\Delta t)) - (u_{7h}(t) - u_{1h}(t)))$$

with a limiting positive value of  $+R_h$  and a limiting negative value of  $-R_h$  imposed both on  $(\bar{F}_{1h}(t+\Delta t))_{\text{nonl.}}$  and on  $(\bar{F}_{7h}(t+\Delta t))_{\text{nonl.}}$ .

## RESULTS OF ANALYSIS

The acceleration time histories of nodes 1, 4 and 6 are shown in Figs. 5 to 7. Also shown are the relative horizontal displacement  $\delta$  between nodes 1 and 7 (Fig. 8) and the sliding code with a value of +1 indicating sliding of the upper raft toward the right, a value of -1 indicating sliding toward the left and a value of 0 indicating no sliding (Fig. 9). Although sliding occurs at very few occasions and over short periods of time, the peak accelerations in the superstructure are substantially lower than when using a non-sliding isolation mechanism. This is shown in Table 1. Also shown in Table 1 is the case where the upper raft is rigidly connected to the lower raft, i.e. the case in which no isolation mechanism is introduced. The associated peak accelerations are then generally still larger.

**Table 1: Peak response values for various isolation mechanisms**

isolation mechanism	$(\ddot{u}_{1h})_{\text{max}}$ m/sec**2	$(\ddot{u}_{4h})_{\text{max}}$ m/sec**2	$(\ddot{u}_{6h})_{\text{max}}$ m/sec**2	$(\delta)_{\text{max}}$ cm
sliding	1.30	2.19	1.52	14.5
non-sliding	1.97	3.53	2.51	6.4
none	3.29	4.21	2.32	----

As indicated earlier, one can solve nonlinear soil-structure-interaction problems by disregarding the frequency dependence of the stiffness coefficients of the foundation. The peak accelerations obtained when introducing this approximation are shown in Table 2. The constant spring coefficients are selected as the zero-frequency values of the actual dynamic spring coefficients and the constant damping coefficients are taken equal to the infinite-frequency values of the actual dynamic

damping coefficients. Differences in peak accelerations are observed. Similar differences are also observed when analyzing the same superstructure with isolation mechanism resting on a softer soil ( $C_s = 150$  m/s for the layer and  $C_s = 300$  m/s for the halfspace) and on a stronger soil ( $C_s = 600$  m/s for the layer and  $C_s = 1200$  m/s for the halfspace).

**Table 2: Peak response values with/without frequency dependence (various soils)**

soil	frequency dependence	$(\ddot{u}_1)_{max}$ m/sec**2	$(\ddot{u}_4)_{max}$ m/sec**2	$(\ddot{u}_6)_{max}$ m/sec**2	$(\delta)_{max}$ cm
medium	yes	1.30	2.19	1.52	14.5
	no	1.37	2.37	1.61	15.8
soft	yes	1.77	2.49	1.64	4.4
	no	1.74	2.81	1.80	5.8
strong	yes	1.27	2.15	1.44	13.3
	no	1.31	2.24	1.47	13.6

The peak accelerations are generally lower when considering the frequency dependence of the stiffness coefficients of the soil than when disregarding it. It should however not be concluded, from these data, that disregarding this frequency dependence and using constant spring and damping coefficients leads to a conservative design. The above results apply only to the specific superstructure, isolation mechanism and sites investigated and do not form a large enough data base from which a general conclusion can be drawn.

## CONCLUSIONS

This paper addresses the calculation of the global seismic response of a reactor building on a sliding-type base isolation which interacts with the surrounding semi-infinite soil. Two major conclusions are drawn from this study.

First, the HFTD procedure proves to be very effective in performing a nonlinear seismic analysis in which the frequency dependence of the stiffness coefficients of the soil is duly accounted for. The accuracy of the results is thus the same as the accuracy achieved in a linear analysis in which this frequency dependence is routinely considered.

Second, the comparison between the peak accelerations of selected nodes when accounting for the frequency dependence of the stiffness coefficients of the soil and when disregarding it shows that the results of the analysis are influenced by this frequency dependence. In the present case, this influence is however limited (difference in peak accelerations between 2% and 13%). This is not surprising as the purpose of an isolation system is to isolate the superstructure from the surrounding soil. Any reasonable changes in soil properties or modeling thereof thus does not strongly affect the calculated response of the superstructure.

## ACKNOWLEDGMENT

The support of the Swiss National Science Foundation under grant No. 82.598.0.88 is gratefully acknowledged.

## REFERENCES

- Darb're, G.R. and Wolf, J.P (1988a). Criterion of Stability and Implementation Issues of Hybrid Frequency-Time-Domain Procedure for Nonlinear Dynamic Analysis. *Earthquake Engineering and Structural Dynamics*, Vol. 16, 569-581.
- Darb're, G.R. (1988b). Hybrid Frequency-Time-Domain Procedure for Nonlinear Dynamic Analysis with Application to Nonlinear Soil-Structure Interaction. *9th World Conference on Earthquake Engineering*, Tokyo/Kyoto.
- Kawamoto, J.D. (1983). Solutions of nonlinear dynamic structural systems by a hybrid frequency-time-domain approach. *Research Report R83-5*, Massachusetts Institute of Technology, Department of Civil Engineering, Cambridge.

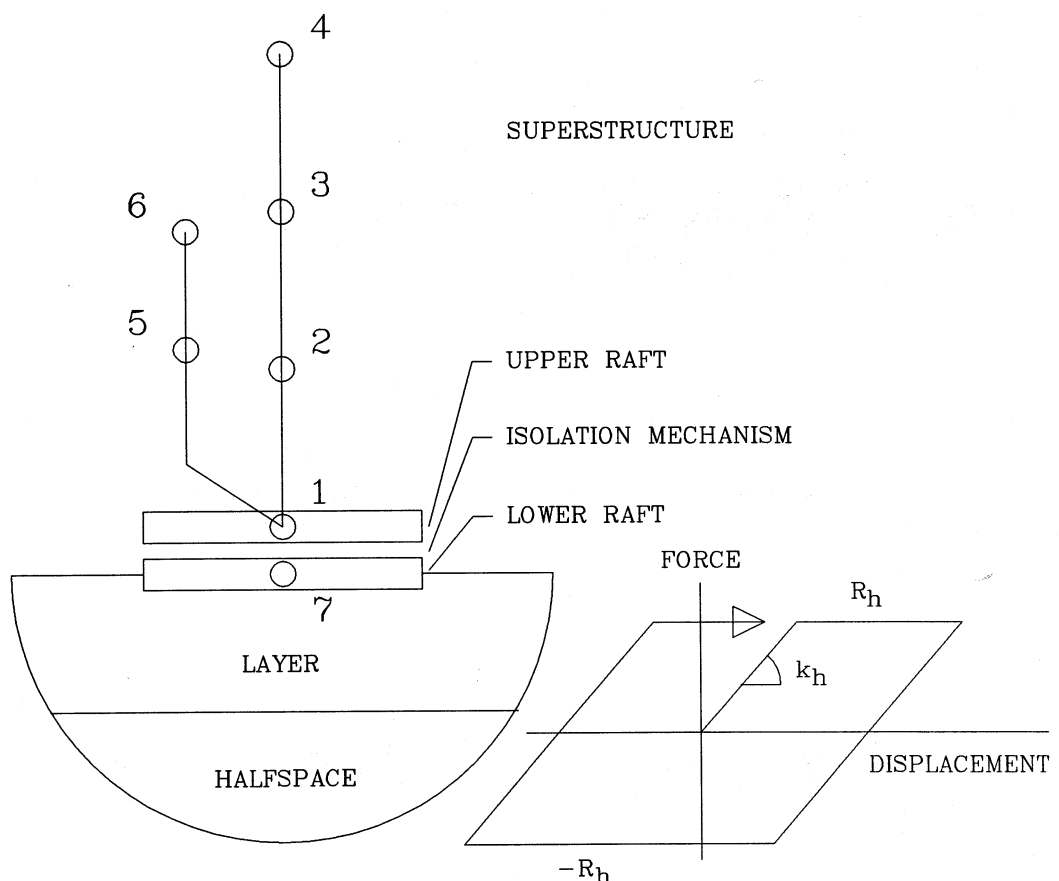


Fig. 1 - Two-dimensional model

Fig. 2 - Horizontal force/  
displacement relation  
of isolation mechanism

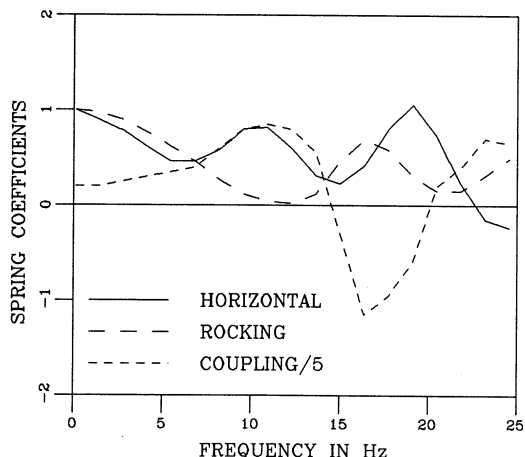
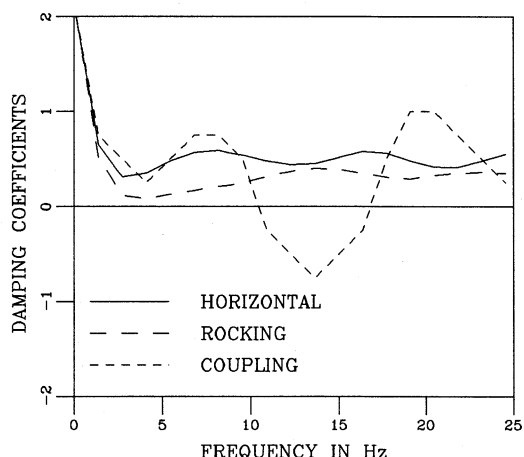


Fig. 3 - Dynamic stiffness coefficients of massless circular rigid foundation  
a) spring coefficients



b) damping coefficients

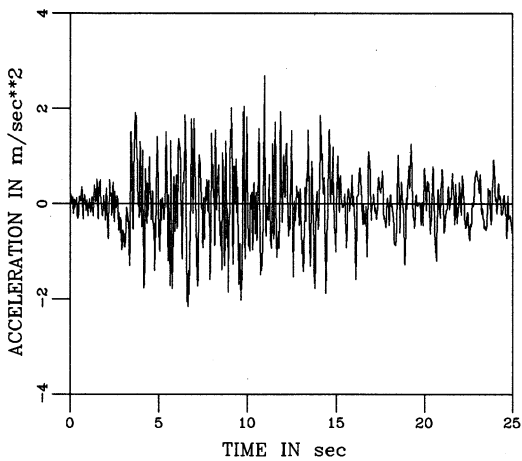


Fig. 4 - Earthquake input acceleration

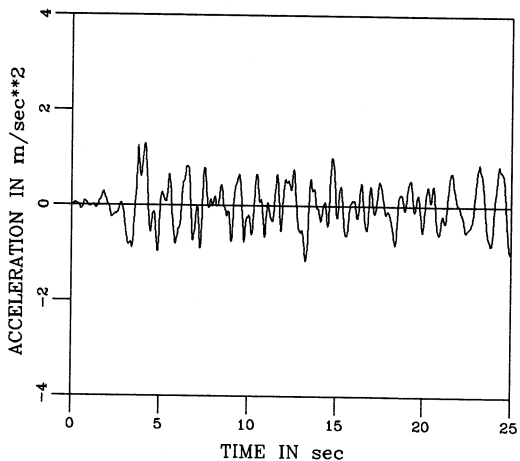


Fig. 5 - Horizontal acceleration of node 1

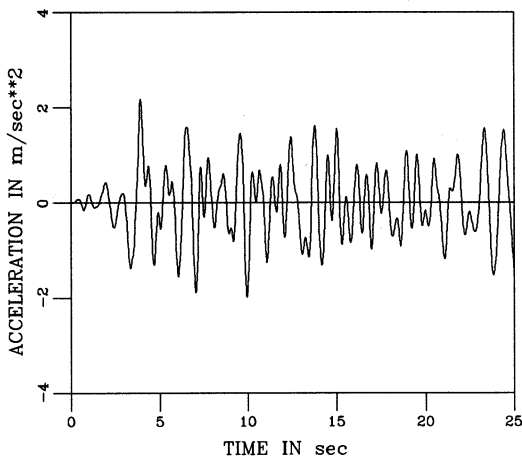


Fig. 6 - Horizontal acceleration of node 4

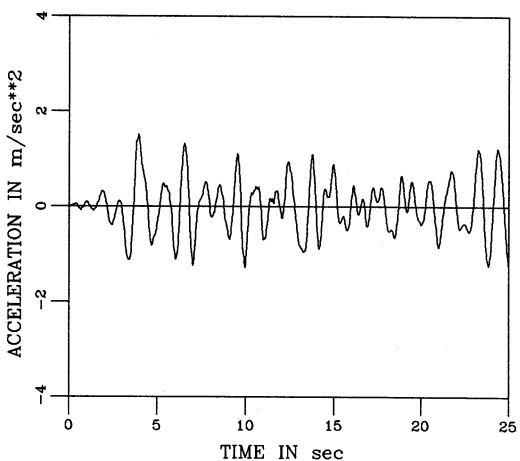


Fig. 7 - Horizontal acceleration of node 6

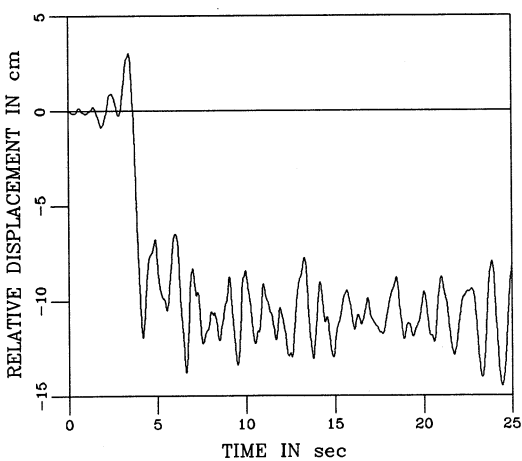


Fig. 8 - Relative isolation displacement

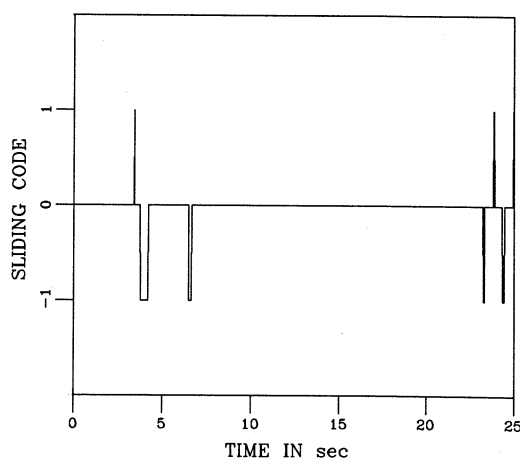


Fig. 9 - Sliding code for isolation mechanism